Regime shift caused by accelerated density reorganization on the Weddell Sea continental shelf with high-resolution atmospheric forcing

Vanessa Teske[1], Ralph Timmermann[1], Cara Nissen[2], Rolf Zentek[4], Tido Semmler[1,3], and Günther Heinemann[4]

[1]Alfred Wegener Institute for Polar and Marine Research, D-27570 Bremerhaven, Germany
[2]Department of Atmospheric and Oceanic Sciences and Institute of Arctic and Alpine Research, University of Colorado, Boulder, Boulder, Colorado, USA
[3]Met Éireann, 65-67 Glasnevin Hill, D09 Y921 Dublin, Ireland
[4]Department of Environmental Meteorology, University of Trier, D-54286 Trier, Germany

Correspondence: Vanessa Teske (vanessa.kolatschek@awi.de)

Abstract.

The strong Antarctic Slope Front in the southern Weddell Sea limits the present-day transport of modified Warm Deep Water onto the continental shelf and is associated with a characteristic V-shape in the density structure all along the continental slope. The mechanisms controlling today's V-shape are well studied, but its future development is not yet well constrained. In this study, we run ocean model simulations for a 21st-century Shared Socio-economic Pathways (SSP) 3-7.0 emission scenario forced with atmospheric model output from simulations with a global climate model and from a higher-resolved regional atmospheric model, respectively. We find that the resolution of the atmospheric model component influences the simulated future transport of modified Warm Deep Water onto the continental shelf through differences in the evolution of the depth and symmetry of the V-shape over the 21st century. In both simulations, reduced sea-ice formation and weakened Ekman downwelling reduce the depth of the V-shape and increase the sensitivity of its position above the slope to seasonal variations in sea-ice production and in the wind field. Using data from an atmosphere model with higher resolution leads to an acceleration of the density redistribution on the continental shelf, provoking a regime shift from cold to warm Filchner Trough through a cross-slope current before the end of the 21st century. As cross-slope currents disturb the continuity of the V-shape, we define a grade of connectivity to quantify the lateral integrity of the V-shape along the continental slope. We find that the integrity of the V-shape reduces with a delay of 3 months after a strong cross-slope current of modified Warm Deep Water enters Filchner Trough. Our results also indicate that the SSP3-7.0 climate scenario may have a higher potential for a regime shift than other ocean simulations for the same scenario but with lower atmospheric resolution suggest. Atmospheric downscaling increases the potential for a regime shift, dominated by warmer summer air temperatures. The Antarctic Slope Front is temporarily disturbed by cross-slope currents but the primary reason for the regime shift is the cross-slope density gradient.

1 Introduction

The Filchner Trough on the continental shelf in the southern Weddell Sea, Antarctica (Fig. 1), is one of the key regions of Dense Shelf Water (DSW) export and therefore plays an important role in the global ocean circulation (Heywood et al., 2014). However, the Filchner Trough is also a region where a southward current of modified Warm Deep Water (mWDW), the local cooler derivative of Circumpolar Deep Water, may reach the Filchner ice shelf cavity and significantly increase melt rates (Darelius et al., 2016; Ryan et al., 2020). Future climate projections for different warming scenarios have shown that a regime shift from a cold DSW-dominated to a warm mWDW-dominated Filchner Trough is possible during the 21st century (Timmermann and Hellmer, 2013; Daae et al., 2020; Haid et al., 2023; Nissen et al., 2023; Teske et al., 2024). Numerous studies have demonstrated that the density ratio between the continental shelf and the open ocean is critical in controlling the on-shelf transport of relatively warm off-shore water (Daae et al., 2020; Haid et al., 2023; Nissen et al., 2023). While a higher density of shelf waters prevents a warm inflow onto the shelf, projections have shown the potential for a reversal of the density ratio (Haid et al., 2023; Nissen et al., 2023), allowing for mWDW transport onto the continental shelf.

North of Filchner Trough above or near the continental shelf break sits the Antarctic Slope Front (ASF), the frontal zone between coastal and open-ocean waters which is associated with strong subsurface temperature and salinity gradients. Around Antarctica, the structure of the ASF varies depending on hydrographic properties over the continental shelf and shelf break, and can be classified into three groups: fresh shelf, warm shelf, and dense shelf (Thompson et al., 2018). With its DSW production and export, the continental shelf of the southern Weddell Sea is an example for a dense shelf. For dense shelves, density surfaces tilt down southward towards the continental slope, but shoal again above the DSW layer. This creates a characteristic V-shape running perpendicular to the continental slope (see also Fig. 2a) which has been described in many studies (e.g., Gill, 1973; Ou, 2007; Baines, 2009; Thompson et al., 2018).

Variability in the V-shape has been linked to variability in both DSW export and on-shelf transport of mWDW. While the northern arm of the V-shape is formed by Ekman downwelling (Sverdrup, 1954), the southern arm of the V-shape is formed by entrainment of overlying surface water to the descending flow of DSW (Gill, 1973; Baines, 2009). The V-shape shows seasonal variability in depth that has been associated with variations in the along-shore wind strength (Graham et al., 2013). For example, a peak in wind strength in the southeastern Indian Ocean in April 2009 led to increased mixing, on-shore Ekman transport and convergent downwelling on the continental shelf near 113°E. Similar behaviour was observed in 2010 and 2011 (Peña-Molino et al., 2016). Kida (2011) showed in a numerical model experiment with an idealized set-up of the Filchner Trough and the southern Weddell Sea that enhanced winds lead to a deepening of the V-shape and a decrease of the ocean stratification near the continental shelf break. The larger amount of lighter surface water at greater depth increases the density gradient across the shelf break and enhances the overflow transport. In contrast, three-dimensional eddy-resolving simulations by Stewart & Thompson (Stewart and Thompson, 2015a, b) showed nearly no sensitivity of the DSW export to wind strength. Reanalysis of ship-based observations, argo floats and data from marine mammals showed a steepening of the angle of the northern arm of the V-shape in the southern Weddell Sea in winter and a flattening in summer (Pauthenet et al., 2021; Le Paih et al., 2020). The seasonal variability of the V-shape and the associated thermocline at the continental slope leads to seasonal

pulses of mWDW flowing into the Filchner Trough (Årthun et al., 2012; Hellmer et al., 2017). Several studies have shown that
55   an intensification of these seasonal pulses is a precursor for an impending regime shift in the Filchner Trough (Hellmer et al.,
2017; Naughten et al., 2021; Teske et al., 2024).

Despite its importance for the on-shelf supply of heat governing Antarctic ice shelf melting, only comparatively few studies
with global ocean or climate models have focused on the Antarctic Slope Current or the ASF due to the high resolution
requirements to adequately resolve coastal ocean dynamics (Mathiot et al., 2011; Stewart et al., 2019; Beadling et al., 2022;
60   Huneke et al., 2022). While only Beadling et al. (2022) concentrated on possible responses of the ocean to changes in the wind
field and meltwater input in a future climate, their model resolution of 100 km to 200 km is relatively coarse. Mathiot et al.
(2011) showed that a downscaling of the atmospheric forcing to 40 km in a hindcast scenario increases katabatic winds and
increases the strength of the seasonal cycle in the wind and temperature fields. While modeling studies on different aspects that
affect the Antarctic Slope Current, like freshwater input or changes in the wind strength and direction are more abundant, they
65   often use idealized set-ups, regional models, or are only coarsely resolved (Kida, 2011; Nøst et al., 2011; Dinniman et al., 2012;
St-Laurent et al., 2013; Hattermann et al., 2014; Lockwood et al., 2021; Ong et al., 2023). Previous studies have described a
possible regime shift in the Filchner Trough, but less attention has been paid to the consequences that a shift in the current
regime might have for the density structure at the continental slope which is controlling the mWDW inflow into Filchner Trough
(Hellmer et al., 2012; Timmermann and Hellmer, 2013; Naughten et al., 2021; Nissen et al., 2022, 2023, 2024). The sensitivity
70   of the ocean processes in response to the atmospheric forcing was demonstrated by Hattermann et al. (2014), Haid et al. (2015)
and Dinniman et al. (2015). This leads us to the hypothesis that resolved mesoscale atmospheric processes may intensify the
seasonality of the V-shape, the on-shore mWDW transport and the export of DSW in the Weddell Sea. Additionally, a finer
atmospheric resolution produces more detailed and more pronounced temperature and wind speed gradients mostly related to
katabatic winds and foehn wind (Van Lipzig et al., 2004; Mathiot et al., 2011; Van Wessem et al., 2015; Elvidge et al., 2014;
75   Cape et al., 2015).

The aim of this study is to explore the evolution of the V-shaped ASF in the southwestern Weddell Sea in a warming climate
(for study area see Fig. 1). By using ocean model simulations forced with data from two atmosphere models with different
grid resolutions, we assess the processes governing the structure of the ASF and the transport of mWDW onto the continental
shelf. To reach that goal, we analyse (i) how the cross-slope structure of the V-shape at the Filchner Trough sill develops in a
80   high-emission climate scenario for the 21st century in Chapters 3.2 and 3.3, (ii) the change in seasonal atmospheric variability
and its influence on the symmetry and structure of the V-shape (Chapters 3.4 and 3.5), and (iii) the longitudinal integrity of the
V-shape as an indicator for the stability of the ASF and a possible regime shift in the Filchner Trough in a warming climate
(Chapter 3.6).
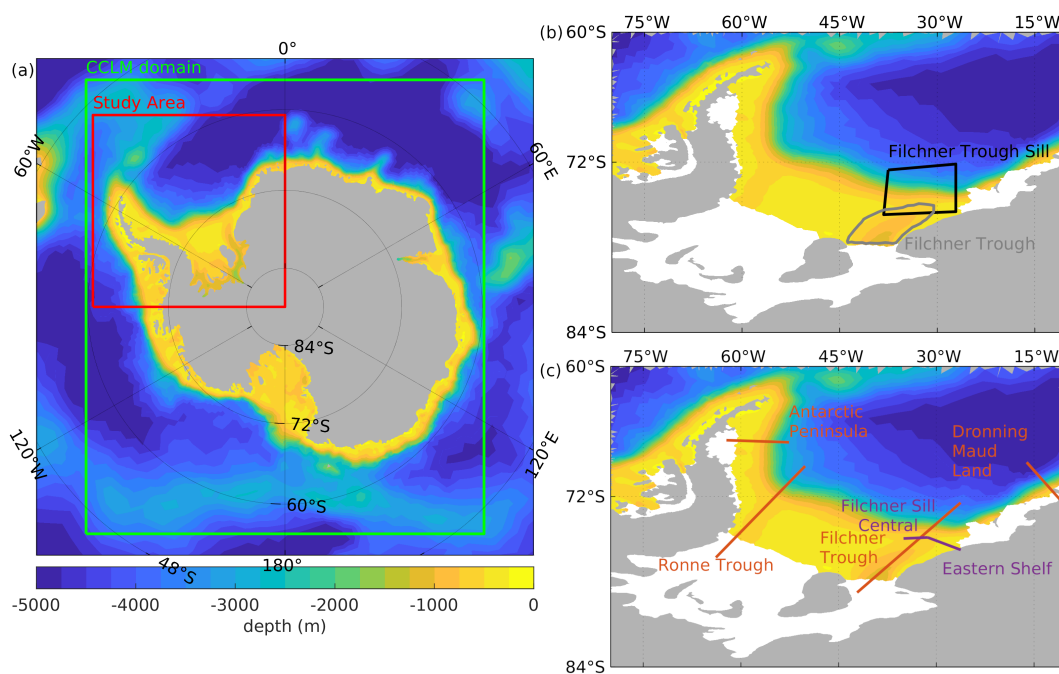
Figure 1. a) FESOM bottom topography in the Southern Ocean, study area in the Weddell Sea (red line) and perimeter of the COSMO-Climate Model (CCLM) domain (green line). b) Location of areas and c) sections used in the analysis of this study. Areas shaded in white represent ice shelves.

2 Methods

2.1 The ocean model FESOM

For this study, we performed ocean model simulations with the Finite Element Sea-ice Ocean Model FESOM-1.4 (Wang et al., 2014). FESOM is a global ocean general circulation model based on unstructured-mesh methods coupled with a dynamic-thermodynamic sea ice component, also including a representation of ice-shelf cavities (Timmermann et al., 2012; Wang et al., 2014; Danilov et al., 2015). The interaction between the ocean and ice shelves is governed by the three-equation system that describes the flux of heat and fresh water through an exchange-controlling boundary layer (Hellmer and Olbers, 1989; Holland and Jenkins, 1999). The variable horizontal resolution of the ocean mesh ranges from (minimum) 4 km around Antarctica and its adjacent ice shelf cavities, via 25 km at 75°S in the Weddell Sea, to 250 km at the equator. In the vertical, the mesh has 99 depth levels (z-levels) of varying thickness (Gurses et al., 2019; Nissen et al., 2023). Here, we perform two ocean model simulations forced with atmospheric data from either a global climate model ("REF" simulation throughout the paper) or a higher-resolved regional atmospheric model (referred to as the "FECO" simulation) which will be described in more detail in the following section.

2.2   The atmospheric forcing data

The FESOM reference simulation (REF) is forced with global atmospheric data created with the AWI Climate Model (AWI-CM), a coupled global climate model using FESOM1.4 as the ocean model and ECHAM6.3.04p1 as the atmospheric model
100   component, as a contribution to phase 6 of the Coupled Model Intercomparison Project (CMIP6; Semmler et al., 2020). The atmospheric data resolution ranges from approx. 27 km to 52 km in zonal direction and corresponds to approx. 100 km in meridional direction. Our ocean model simulation is initialized in the year 2000 with FESOM output from Nissen et al. (2023) and is driven by 3-hourly atmospheric output of the historical AWI-CM simulation for the period 2000 to 2014 and of the future Shared Socio-economic Pathways (SSP) 3-7.0 emission scenario (Meinshausen et al., 2020) projection for 2015 to
105   2100, identical to Nissen et al. (2023).

The FESOM FECO simulation is forced with a regional atmospheric forcing data set which was created with the COnsortium for Small-scale MOdeling - CLimate Mode model (COSMO-CLM or CCLM; Steger and Bucchignani, 2020; Zentek and Heinemann, 2020), a regional non-hydrostatic atmospheric model with terrain-following vertical coordinates at a horizontal resolution of 15 km. The used CCLM is a polar-adapted version including improved parameterizations for sea ice and the
110   stable boundary layer (see Heinemann et al., 2022, for more details). The model is used in a forecast mode with daily re-initialization and a spin-up of 12 hours. The CCLM domain reaches the northernmost corners at approx. 50°S (Fig. 1a). At its lateral boundaries, it is driven by the global AWI-CM data sets described above. Sea ice concentration and thickness are initially taken from FESOM data of the AWI-CM simulation, but are modified by the parameterizations of grid-scale and sub-grid-scale ice in leads and polynyas. For use as forcing for the global ocean model FESOM, the CCLM output is merged with
115   the global AWI-CM atmospheric output. The merging follows the procedure from Haid et al. (2015) and uses a transition zone of 2° to linearly interpolate between the global AWI-CM data and the regional CCLM data. South of this 2° boundary only CCLM data is applied as forcing, while only AWI-CM data is used outside the CCLM domain. Inside the transition zone, the weighted average depending on the distance to the CCLM domain boundary is used. CCLM data are available for the three timeslices 2000-2014, 2036-2050, and 2086-2100. The following quantities are used from the downscaled CCLM simulations:
120   2m-temperature, 10m-wind, downward longwave and shortwave radiation at the ocean surface, mean sea level pressure, 2m specific humidity and total precipitation. We ran FESOM simulations forced with CCLM (henceforth called FECO) for each of the three time slices, each preceded by 10 years of spin-up, already driven by the CCLM data (2000-2009, 2036-2045, and 2086-2095, respectively). The spin-ups were branched off the REF simulation in 2000, 2036, and 2086, respectively.

2.3   Grade of Connectivity

125   We define the grade of connectivity (GOC) as a metric describing the coherency of the V-shape along the continental slope in a selected sector (here the Filchner Trough Sill, see Fig 1b). Motivated by the link between the V-shape and DSW export from the Weddell Sea continental shelf (Gill, 1973; Baines, 2009; Nissen et al., 2022) and on-shelf mWDW transport (Nøst et al., 2011; Stewart and Thompson, 2015a; Thompson et al., 2018), this metric quantifies the modification (or erosion) of the V-shape structure in response to cross-slope currents. The GOC is defined as the normalized zonal mean of the north-south
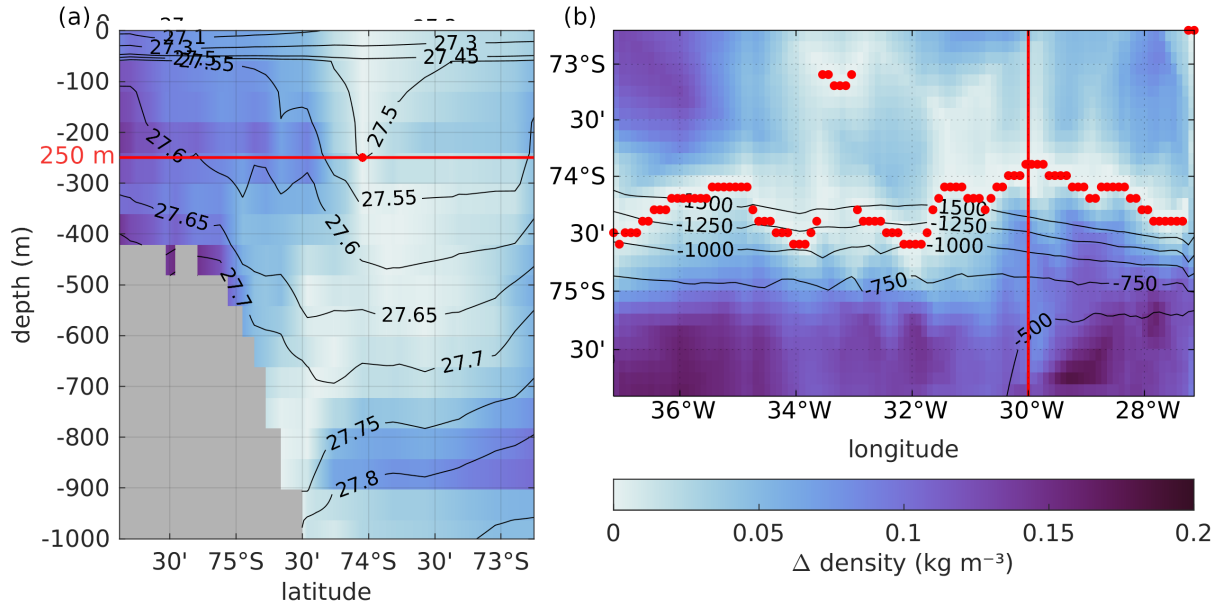
Figure 2. Section across Filchner Trough sill of the horizontal potential density distribution relative to the level-wise horizontal minimum density in December 2000 to illustrate the connection between the V-shaped density distribution and the grade of connectivity as defined in section 2.3. Isolines depict the potential density in kg m^{-3} relative to 1000 kg m^{-3}. The red dot marks the location of the minimum density difference at 250 m depth, the horizontal line the position of the level presented in (b). (b) Horizontal projection of the density difference at 250 m depth with bottom isobaths. Red dots mark the location of the meridional minimum in longitudinal increments of 0.1°. The red line marks the location of the section shown in panel (a).

130 variations of the deepest point of the V-shape in a horizontal plane. To calculate the GOC, we first interpolate the model data from the unstructured grid to a regular grid with a resolution of 0.1° through linear interpolation between FESOM grid points. As a second step, to find the meridional position y_n of the deepest point of the V-shape for each longitude coordinate, we find the horizontal density minimum at the chosen depth by searching for the maximum density difference at 250 m depth compared to the northern border of the selected area (here 72.69°S; Fig. 2). Δy_n then denotes the absolute meridional distance from the

135 neighboring y_n. The average GOC is then calculated from monthly mean model output as

$$GOC = \frac{1}{n} \sum_n \begin{cases} 1, & if \ \Delta y_n \leq d_L \\ \frac{d_L}{\Delta y_n}, & if \ \Delta y_n > d_L \end{cases} \tag{1}$$

where n is the number of grid cells in zonal direction, and the distance threshold $d_L = 0.2°$ is the maximum distance that counts two neighbouring density minima as connected. In summary, the GOC is defined as the normalized zonal mean of the north-south variations of the deepest point of the V-shape in a horizontal plane. We normalize by n so that it gives a number between 0 and 1, with lower values indicating a less coherent V-shape along the continental slope and a value of 1 indicating a

V-shape without disruptions in longitudinal direction. As such, the GOC allows for a quantitative description of the slope front stability and a quantitative assessment of how this relates to, e.g., on-shelf transport of mWDW.

3 Results

3.1 Present-day V-shape in the Weddell Sea (REF simulation)

145 The reference simulation REF shows a distinct wedge structure of the isopycnals above the continental slope for the period 2010-2014, but details vary substantially across different sectors of the Weddell Sea (Fig. 3). In the following, the potential density is always given relative to 1000 kg m^{-3}. At the coast of Dronning Maud Land (DML) in the eastern Weddell Sea, a fresh-shelf region, the narrow continental shelf prevents the accumulation of large amounts of DSW. Cold, fresh surface water is pushed towards the coast and subducted, pressing down on the isopycnals of greater density (Fig. 3a). The planes of equal

150 density dip towards the continental shelf and the coast, forming only the northern arm of a V-shape. The section at Filchner Trough (Fig. 3b), a dense-shelf region, shows a strongly pronounced V-shape in which the 27.7 kg m^{-3} isopycnal is found at approx. 500 m greater depth above the continental slope than on the continental shelf. The southern arm of the V-shape is pronounced in the Filchner Trough, as this is an area of DSW overflow (Fig. S1). Further to the west at the Ronne Trough (Fig. 3c), water of colder temperature reaches deeper than at the Filchner Trough. However, the V-shape is less pronounced

155 in the upper open ocean, i.e., the region displays a less pronounced northern arm, due to the deepening of the slope current along its path following the continental slope. At the Antarctic Peninsula in the western Weddell Sea (Fig. 3d), a V-shape in the isolines is clearly visible only in the temperature field and for the 27.7 kg m^{-3} isopycnal and higher-density but not for lower-density isopycnals. In addition, mWDW at temperatures around -1°C can be found on the continental Shelf and in the Larsen Ice Shelf cavity originating from Ronne Trough and following the coast northward (Fig. S1a). The Filchner Trough has

160 previously been shown to be an entrance point for mWDW to reach the Filchner Ronne ice shelf (e.g. Foldvik et al., 1985; Ryan et al., 2017). Because of its particular relevance, we will focus on the Filchner Trough in our further analysis.

3.2 Present-day seasonality of the V-shape at Filchner Trough (REF simulation)

Previous studies have shown that seasonal variations in the density distribution at the continental shelf break control the on-shore flow of mWDW (e.g. Teske et al., 2024). During the historical 2010-2014 time period in REF, the depth and steepness

165 of the V-shape shows seasonal variations (Fig. 4). More intense sea-ice formation on the continental shelf leads to thicker sea-ice above the continental shelf (Fig. S3) and stronger DSW export in winter and spring than in summer and autumn, which pushes down the isopycnals at the continental slope by approx. 50 m (Fig. 4 a, b). This is consistent with observed variations in the thermocline depth at the Filchner Trough sill (Hattermann, 2018), though with a smaller amplitude than in the observations. Sea-ice melting during summer reduces the steepness of the arm of the V-shape above the continental

170 shelf (Fig. 4c). Subsequently, stronger densification over the continental shelf through sea-ice formation in autumn strengthens the southern arm again (Fig. 4d). Sea-ice formation in winter is particularly pronounced along the coasts of the Weddell Sea
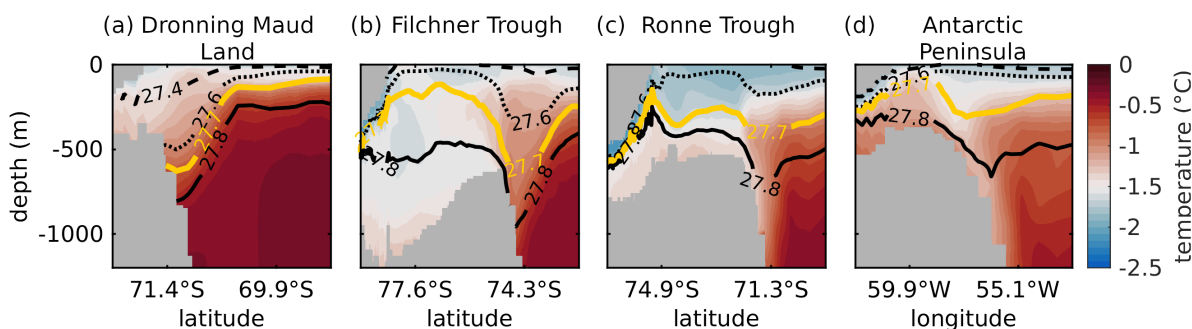
Figure 3. Potential temperature sections across the continental slope in the southern Weddell Sea with isopycnals shown relative to 1000 kg m^{-3} for 27.4, 27.6 27.7 (orange) and 27.8 kg m^{-3} for the average over 2010-2014 in REF. a) Dronning Maud Land, b) Filchner Trough, c) Ronne Trough, and d) Antarctic Peninsula. The continent and ice shelves (marked in grey) are on the left-hand side for all panels. See Figure 1 for the exact locations of the transects.

(Fig. S2e), while in summer most of the Weddell Sea is dominated by sea-ice melting (Fig. S2i). Only a small band along the Filchner-Ronne Ice Shelf edge produces sea ice year round, which - together with sea-ice deformation by tides and variable winds - leads to a band of exceptionally thick sea ice north of Ronne Ice Shelf in summer (Fig. S3i).

175   The rise of the thermocline in summer also enables seasonal pulses of mWDW to flow onto the continental shelf (see also Ryan et al., 2020; Teske et al., 2024). The horizontal temperature gradient in 300 m depth is strongest during winter - which is consistent with observations (Fig. S4; Pauthenet et al., 2021) - however the northern arm of the V-shape has its steepest angle during summer (blue line in Fig. S5). During summer, reduced DSW export (Fig. S6) and weakened Ekman downwelling (see also Fig. 7) reduce the depth of the V-shape compared to winter (Fig. 4c). The main mechanisms behind the seasonal variations

180   are thus the seasonal production of DSW and seasonally varying Ekman downwelling. These mechanisms as found in the simulation agree with observations and previous modelling studies (Peña-Molino et al., 2016; Le Paih et al., 2020; Pauthenet et al., 2021; Ryan et al., 2020).

3.3   Effect of a warming climate on the seasonally varying V-shape geometry (REF simulation)

Over the 21st century, increased summer sea-ice melting and reduced freezing rates in winter above the continental shelf
185   (Fig. S2) lead to freshening of the continental shelf and to a density redistribution in the Filchner Trough and across the continental slope. While the geometry of the V-shaped density distribution is mostly symmetrical in 2010-2014 (Fig. 4), it becomes lopsided towards the end of the century in the REF simulation (Fig. 5). A reduction of the density over large parts of the water column in Filchner Trough by up to 0.2 kg m^{-3} between 2000 and 2100 reduces the vertical extent of the southern arm of the V-shape. In addition, a shoaling of the slope current over the course of the century reduces the depth of the V-shape
190   so that the yearly mean depth of the 27.8 kg m^{-3} isopycnal lifts from approx. 992 m to 791 m between 2010-2014 and 2096-2100 (dotted and dashed horizontal lines in Fig. 5, respectively). Of all seasons, the V-shape reaches its deepest position in summer by the end of the century (Fig. 5c), as opposed to in winter for the 2010-2014 period (Fig. 4).
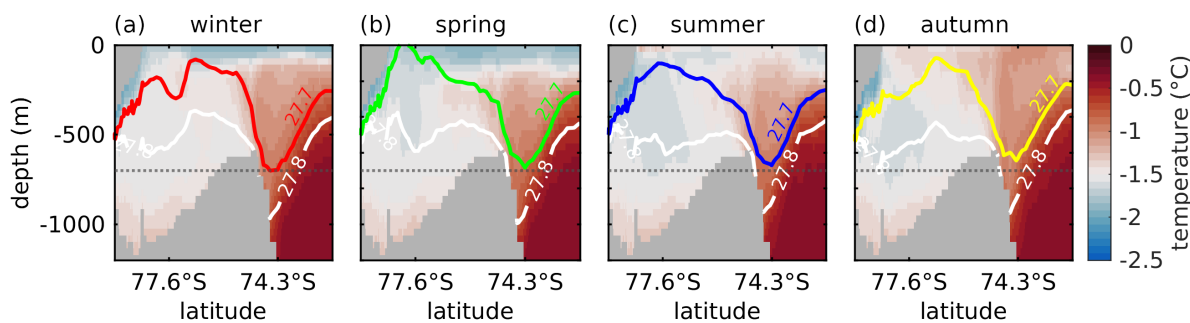
Figure 4. Potential temperature in the 2010-2014 mean of the Filchner Trough section in REF for winter (June-August), spring (September-November), summer (December-February), and autumn (March-May). The colored (white) lines show the position of the 27.7 kg m^{-3} (27.8 kg m^{-3}) isopycnal in the respective season. Horizontal dotted line shows the maximum depth of the 27.7 kg m^{-3} isopycnal in winter. The continent and ice shelves (marked in grey) are on the left-hand side for all panels. See Figure 1 for the exact locations of the transects.
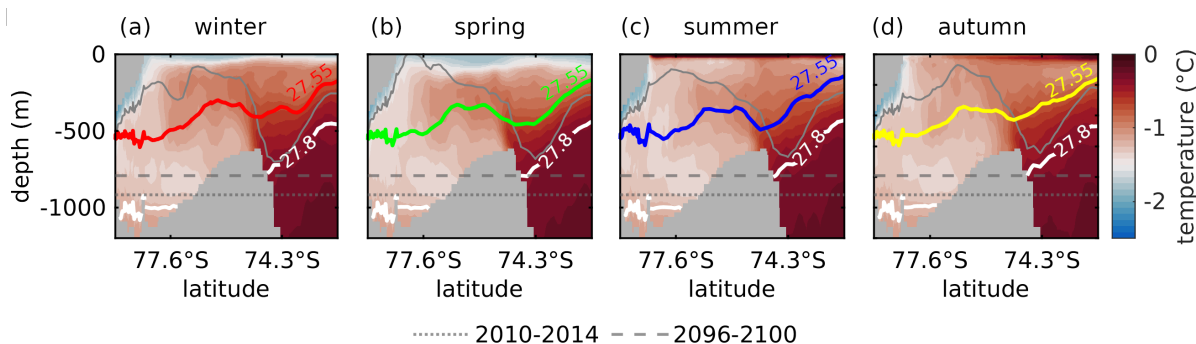
Figure 5. Potential temperature in the 2096-2100 mean of the Filchner Trough section in REF for a) winter (June-August), b) spring (September-November), c) summer (December-February), and d) autumn (March-May). The colored lines show the position of the 27.55 kg m^{-3} isopycnal in the respective season, the white line the 27.8 kg m^{-3} isopycnal. The gray line shows the position of the 27.7 kg m^{-3} from Fig. 4. The dotted (dashed) horizontal gray line shows the mean depth of the 27.8 kg m^{-3} isopycnal in the multi-year mean of 2010-2014 (2096-2100).

The change in sea-ice thickness and concentration (Fig. S7a & b) during the 21st century does not only lead to freshening of shelf waters, but also influences how the wind field impacts the ocean surface. To isolate the relative effects of wind speed changes and changes in sea-ice properties, we compute the wind stress curl from the 2m wind field assuming a constant drag coefficient over ocean (C_{AO}=1.00e-3) and sea ice (C_{AI}=1.32e-3), weighted by sea ice concentration per grid cell. We find that an intensification of the wind field towards the end of the century enhances existing wind stress curl patterns in winter (Fig. 6a-d), while qualitatively the patterns remain largely unchanged. In contrast, considering the ocean surface stress, i.e. taking the effect of the sea-ice cover into account, we find an alternating pattern of negative and positive surface stress curl, corresponding to alternating areas of up- and downwelling, respectively (Fig. 6e). With a reduction of winter sea-ice thickness by up to 80%

compared to at the beginning of the century, some of the up- and downwelling areas are redistributed. Regional variability is slightly reduced so that the surface stress curl resembles the wind stress curl more closely at the end of the century. Similar changes in the wind stress curl can be seen in spring and autumn (Fig. 6 b/d vs. f/h). In summer, when the sea-ice thickness (Fig. S2) and concentration (not shown) in the Filchner Trough is already low between 2010 and 2014, a southward shift of

205 the wind field increases areas of downwelling above the continental slope. The impact of sea ice on the surface stress curl is especially visible in autumn where in the 5-year average for March to May, the Filchner Trough is covered approximately halfway by sea ice. South of approx. 76°S, sea ice creates alternating patterns of positive and negative surface stress curl, while north of this, surface stress curl closely resembles the wind stress curl (Fig. 6 d, h).

From the fact that in the comparison between 2096-2100 and 2010-2014 we find modified patterns of spatial variability

210 in the ocean surface stress curl (lower panels in Fig. 6) much more pronounced than in the wind stress curl (upper panels in Fig. 6), we conclude that the long-term trend in up- and downwelling patterns is created by trends in the sea ice cover rather than in the wind field. The combination of reduced DSW export in winter and spring and the enhanced wind stress impact on the ocean is then responsible for the change in the seasonal variations of the V-shape.
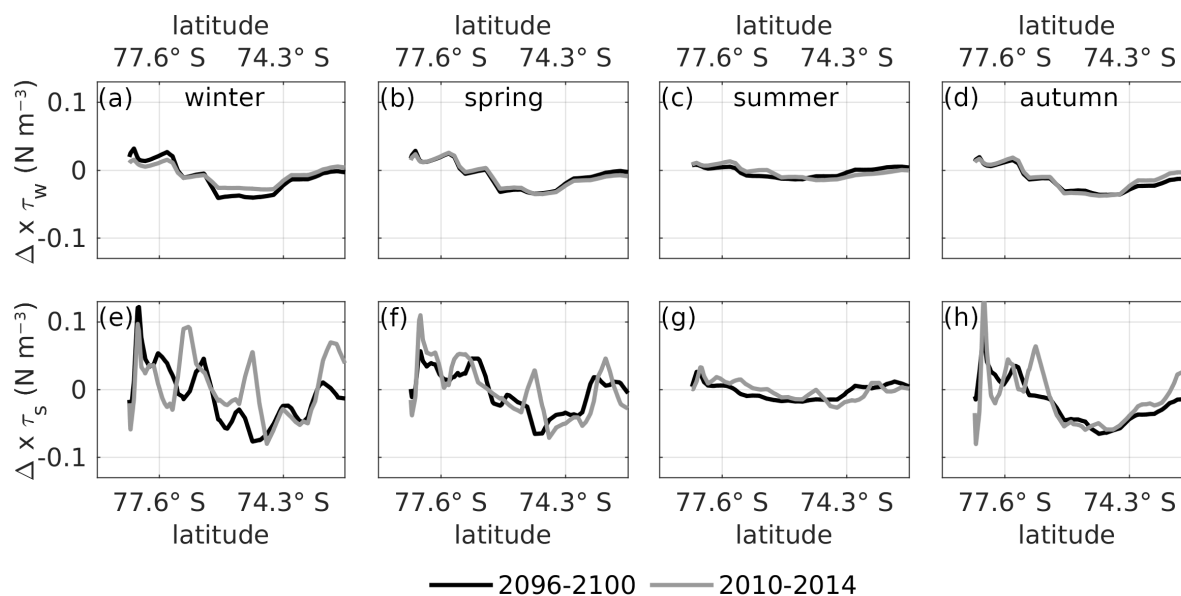
Figure 6. Wind stress curl ($N\,m^{-3}$), estimated from the 2m-wind field, in the 5-year means of 2096-2100 (black line) and 2010-2014 (gray line) in REF above the Filcher Trough section (see Fig. 1) for (a) winter (June-August), (b) spring (September-November), (c) summer (December-February), and (d) autumn (March-May). (e)-(h) Same as (a)-(d) but for surface stress curl on the liquid ocean from overlying atmosphere and sea ice. Positive curl corresponds to downwelling.
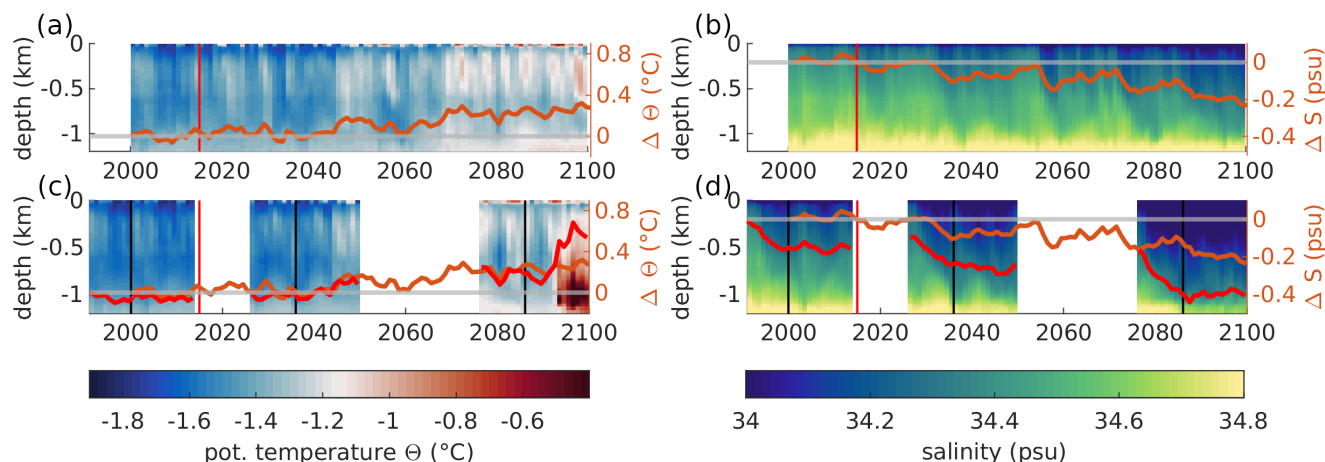
Figure 7. Hovmöller diagram of the yearly mean temperature in Filchner Trough (see Fig. 1) for (a) REF and (c) FECO. Colored lines show the relative temperature change of the horizontally and vertically averaged temperature of the whole water column compared to 2000. (b) & (d) Same as (a) & (c) but for salinity. Orange lines in (c) and (d) are the same as the orange lines in (a) and (b), respectively. Red line marks the relative change of the average temperature/salinity in FECO. Red vertical line: boundary between historical and future climate scenario. Black vertical lines: boundary between transition time and experiment in FECO.

3.4 Sensitivity of the Filchner Trough circulation to atmospheric forcing

215 The application of the regional higher-resolved CCLM forcing in FECO affects the transport of mWDW onto the continental shelf. Reduced freezing rates along the coasts in winter and higher melt rates in summer (Fig. S2) due to higher air temperatures (not shown) compared to REF lead to an additional decrease of the Filchner Trough mean salinity by up to 0.2 psu over the course of 10 years of transition time, converging to a new mean state for all three time slices (Fig. 7d). Additionally, lower wind speeds in most of the southern Weddell Sea reduce the wind stress on sea ice and ocean, except for some areas at the

220 eastern Ronne Ice Shelf Front and the Filchner Ice Shelf, where stronger off-shore winds dominate. In contrast to the salinity, the mean potential temperature does not appear to be sensitive to the forcing change (Fig. 7c) in the transition time. In the FECO experiment, the circulation across the Filchner Trough sill and in the trough experiences a regime shift that REF does not. In 2093, mWDW enters the Filchner Trough as a near-bottom current across the sill, strongly increasing the temperature in the trough (Fig. 7c). This is not the first occasion for mWDW to influence the temperature of the Filchner Trough. Over

225 the course of the 21st century, REF shows increasingly stronger seasonal pulses of mWDW crossing into the Filchner Trough across the shelf east of Filchner Trough and along the eastern slope of the trough (Fig. S8). Over the course of the reference simulation, we find an increase in the temperature of the mWDW pulses, originating in a warming of the slope current. The slope current shows a warming trend of approx. 0.053°C per decade between 2000 and 2100. This agrees well with the 0.05°C per decade that were observed between 1980 and 2010 (Schmidtko et al., 2014). Previous studies have suggested that warmer

230 and longer-lasting pulses can be a precursor for a regime shift in the Filchner Trough from a DSW-dominated to a mWDW

dominated state (Timmermann and Hellmer, 2013; Timmermann and Goeller, 2017; Ryan et al., 2020; Nissen et al., 2023; Teske et al., 2024), but despite the increase in the mean temperature and the visible mWDW pulses, no sudden warming of the trough occurs in REF.

Before the regime shift in FECO, the reduced density of the upper 1000 m in the open ocean leads to changes in the position
235 and symmetry of the V-shape above the continental slope (Fig. 8). The comparison of the seasonal positions of the deepest point of the 27.4 kg m^{-3} isopycnal in FECO for 2088-2092 (Fig. 8b) - chosen for its position at depth above the continental slope at all times, but nearly no intersection with the surface in REF - yields an additional horizontal component to the seasonal depth variation seen in REF (Fig. 8a). This horizontal movement displaces the V-shape by approx. 50 km between summer, when the deepest point of the V-shape is at its southernmost point, and winter. The deepest point of the V-shape is closest to
240 the sill in summer and furthest away in winter (Fig. 8b). In addition, the V-shape reaches its deepest position in spring and summer, while REF reaches the deepest point in winter and spring. The fresher water masses on the continental shelf in FECO cause the southern arm of the V-shape to be very flat and to vanish during autumn (Fig. 8b, yellow curve). Stronger Ekman downwelling in autumn, but a late onset of the freezing season lead to a situation that temporarily resembles fresh-shelf regions like the Dronning Maud Land section (Fig. 3d), though sea-ice formation in winter regularly restores the V-shape.

245 ### 3.5 Accelerated density redistribution with high-resolution atmospheric forcing

The high-resolution atmospheric forcing does not only affect the slope front symmetry and seasonality, but also accelerates the reduction of density over the 21st century compared to REF (Fig. 9). The differences in the density evolution between REF and FECO are particularly large in Filchner Trough (Fig 9a). Here, the application of CCLM forcing leads to a negative density trend between 2000 and 2092 that is 1.47 times larger than in REF. Values after 2092 were excluded from the calculation due to the
250 impact the regime shift has on the density of the Filchner Trough. In contrast, above the continental slope north of the Filchner Trough sill, the trend is slightly smaller in FECO than in REF (-1.5 kg m^{-3} century^{-1} as compared to -1.6 kg m^{-3} century^{-1}; Fig. 9b). Separately assessing the trends in temperature and salinity reveals that the density trend on the continental shelf is driven by freshening, while the trend in the slope current is driven by a combination of warming and freshening (Fig. S9). From this we conclude that reduced sea-ice formation is not the only factor influencing the density distribution across the continental
255 slope, but the dominating one for the existence of the V-shape.

3.6 Influence of cross-slope currents on the V-shaped density distribution

With the onset of the near-bottom current of mWDW entering the Filchner Trough in FECO in 2093, the V-shaped density distribution at the continental slope experiences pronounced structural changes that lead to the loss of the southern arm of the V-shape. Visible as a sudden increase in the average temperature in the Filchner Trough (Fig. 7c), the inflow of mWDW in FECO
260 in 2093 brings the bottom density in the Filchner Trough closer to that of the slope current. This has the effect of increasing the stratification of the water column. In combination with low sea-ice formation rates and reduced mixing (not shown) during the freezing season, the seasonal variations in the southern arm of the V-shape vanish at depths below approx. 450 m (Fig. 8d), in contrast to REF, where the V-shape is formed also at greater depths (Fig. 8c). Seasonal variations of the depth of the V-shape
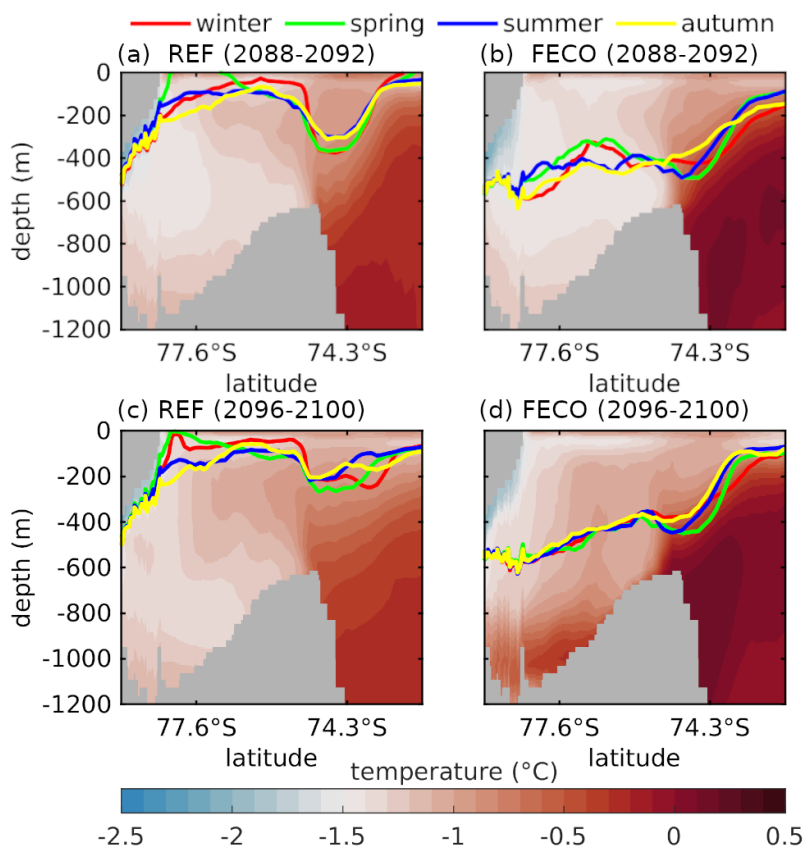
Figure 8. Potential temperature in the 2088-2092 mean (5 years before regime shift in FECO) in a) REF and b) FECO. Colored lines show the position of the 27.4 kg m^{-3} isopycnal. c) and d) same as a) and b) but for 2096-2100.

and the position of the northern arm remain, however, the southern arm of the V-shape decreases strongly in vertical extent.

265 From a height difference in spring of approx. 200 m between the deepest point of the V-shape and the shallowest point above the continental shelf, the 27.4 kg m^{-3} isopycnal position reduces to a vertical range of approx. 80 m after the bottom current onset. With the near-bottom inflow of mWDW into the trough, the sensitivity of the southern arm of the V-shape to sea ice formation is reduced, while the northern arm, which is created by the wind, remains.

The timing of the intensified mWDW flux in FECO can be related directly to the density gradient across the Filchner Sill and

270 the depth of the thermocline at the sill. In FECO, the thermocline remains above the Filchner Trough sill depth throughout the 15-year FECO simulation and stays between 400 m to 600 m depths, while the thermocline in REF rises from approx. 1000 m in 2000 to 600 m depth over the course of the 21st century (last 15 years shown in Fig. 10a). The sill depth of approx. 600 m (horizontal gray line in Fig. 10a) is only crossed occasionally and never for an extended period of time. Despite the thermocline in FECO already reaching above the sill from the beginning of the time slice 2086-2100, the warm near-bottom current is still

275 only developing at a later date. This agrees with the conclusions presented by Haid et al. (2023) suggesting that another key
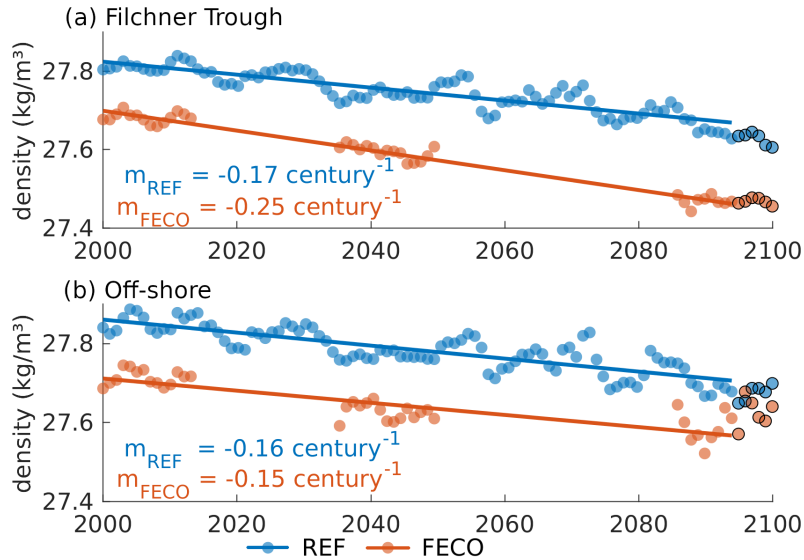
Figure 9. Linear regression of the annual mean potential density relative to 1000 kg m^{-3} over time in a) the Filchner Trough and b) at the Filchner Trough Sill at 636 m depth for REF in blue and FECO in red. The slope of each linear fit is given in the figure. Data points outlined in black were excluded from the calculation due to the regime shift in 2093. The areas over which properties are averaged for the time series are indicated in Fig. 1.
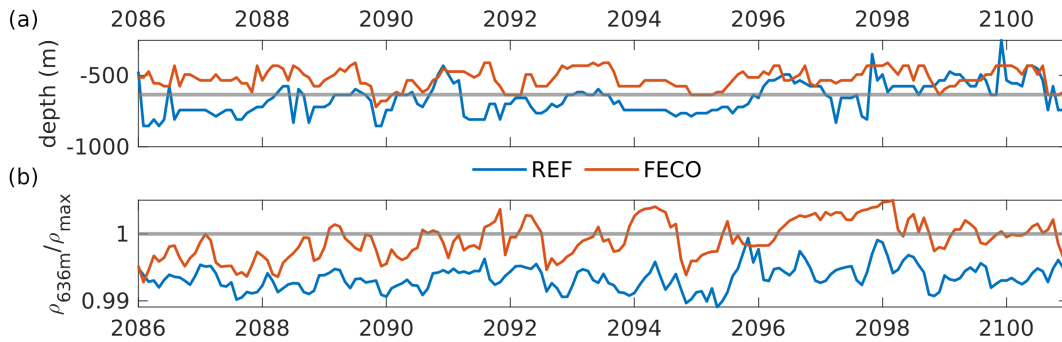
Figure 10. a) Depth of the thermocline at the Filchner Sill (horizontal line: sill depth at 636 m) and b) density ratio between the maximum density in Filchner Trough (ρ_{max}) and the mean density at the Filchner Trough sill (see Fig. 1) at 636 m depth (ρ_{636m}).

factor for or against an inflow of mWDW onto the continental shelf in addition to the depth of the mWDW at the slope is the density ratio between the dense water on the shelf and the slope current (see also Nissen et al., 2023).

The inflow of mWDW onto the continental shelf is not only visible in the cross-slope density structure, but also as a disruption of the V-shape in along-slope direction. In both simulations, the GOC at the Filchner Sill shows multiple minima between 280 2086 and 2100, demonstrating phases of instability of the Antarctic Slope Front where the barrier across the sill is weakened

(Fig. 11). However, not all of the recognised events of a minimum GOC are related to an increased flow of mWDW into the Filchner Trough. The comparison of the southward mWDW (Θ >-0.8°C) transport in the Filchner trough across the central Filchner Trough sill with the GOC in FECO shows a significant correlation with a lag of 3 months (p=0.0005, r=0.35) between the maximum mWDW transport and a minimum of the GOC after 2093 (Fig. 11). In REF, there is not only a lagged correlation between the inflow of mWDW with the GOC (p=7e-7, r=0.36) but also weakly between the outflowing DSW (Θ <-0.8°C) and the GOC (p=0.0001, r=0.29), while FECO does not show this correlation (p=0.27, r=0.08). The calculation of the GOC was performed for 250 m depth, where the V-shape is present at all times, even when it is less pronounced. The changing circulation patterns associated with the density reorganization on the shelf in FECO decouple the weak correlation between the water export and GOC that can be found in REF.
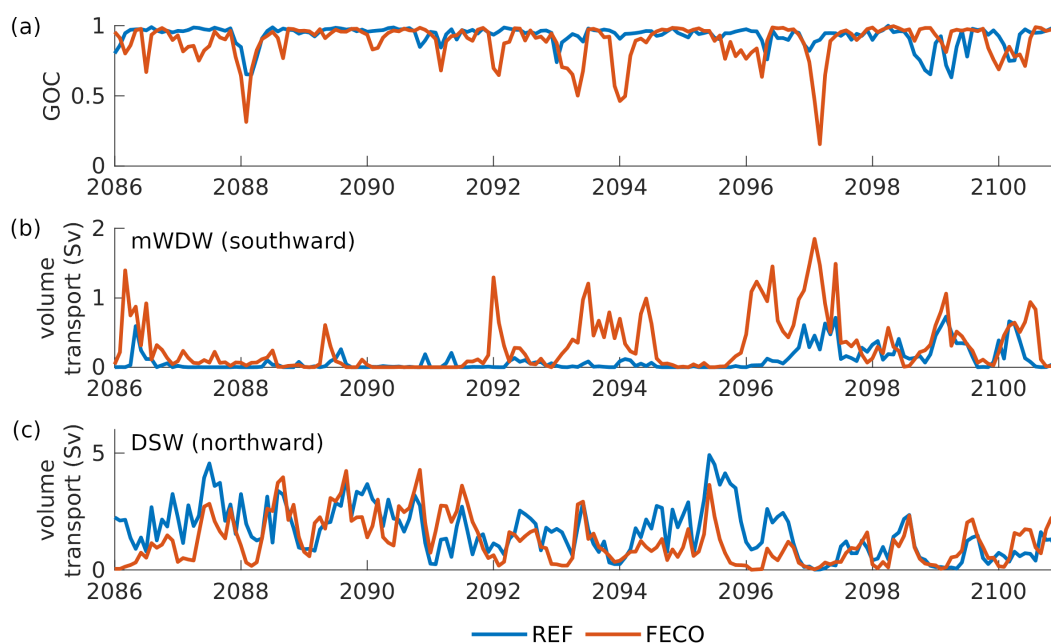
Figure 11. a) Time series of the grade of connectivity (GOC) of the V-shaped density structure above the continental slope at the Filchner Trough sill for REF (in blue) and FECO (in red; for area outline see Fig. 1; for calculation see section 2.3). b) Southward volume transport in Sv across Filchner Sill Central (see Fig. 1) of water masses mWDW with a potential temperature of Θ>-0.8°C and c) northward volume transport of DSW (Θ<-0.8°C).

4 Discussion

4.1 Drivers of the accelerated density redistribution: wind speed and sea ice

Our results show that for the high-emission scenario SSP3-7.0, lower sea-ice production in a simulation with high-resolution atmospheric forcing data accelerate the density redistribution on the continental shelf of the southern Weddell Sea relative to a simulation with lower-resolution atmospheric forcing. Subsequently, the accelerated density redistribution induces a regime shift in the Filchner Trough area before the end of the 21st century. The regime shift from a DSW-dominated to a mWDW-dominated state is accompanied by the near-loss of the southern arm of the V-shaped density distribution at the continental slope that prominently separates the shelf from the open ocean in today's climate.

The main factors controlling the circulation regime in Filchner Trough are the wind field and sea-ice production (Teske et al., 2024), which directly influence the density distribution on the shelf. The on-shore transport of mWDW, which intensifies in the case of a regime shift, strongly depends on the density ratio across the continental slope at the Filchner Trough sill. This ratio changes faster in FECO than in REF, driven by an accelerated freshening of the continental shelf in response to higher summer temperatures and weaker wind speeds in CCLM. Higher summer air temperatures in FECO compared to REF lead to a stronger decline and local melting of summer sea-ice. Since multi-year mean air temperatures are actually lower in FECO than in REF, this emphasizes the importance of the seasonal cycle.

Weaker wind speeds may have two effects: (i) smaller heat loss to the atmosphere, and (ii) less wind-driven sea-ice transport. Both effects tend to reduce sea-ice production and thus winter brine release in regions that are dominated by freezing and export of sea ice. In contrast, stronger off-shore winds at the Filchner Ice Shelf front in FECO increase the occurrence and width of coastal polynyas that locally cause higher sea-ice production rates. While this could counteract some of the freshening of the Filchner Trough, the net effect appears to be dominated by the weaker off-shore winds in the high-resolution atmosphere model.

In the historical time period between 2010 and 2014, REF produces a steeper, narrower temperature and density gradient across the ASF at 300 m depth during winter than during summer, which agrees with the assessment of the ASF by Pauthenet et al. (2021). According to their study, the ASF forming the northern arm of the V-shape has the smallest meridional extent during winter months, which translates to a strong temperature gradient. The steepening is a result of stronger DSW export in winter. The entrainment of colder, fresher surface water suppresses the isopycnal and forces the isopycnal and thermocline into a steeper position. However, observational data for winter in the ice-covered southern Weddell Sea are scarce, leading to high uncertainties in the assessment of the position and extent of the ASF in the southern Weddell Sea. Additionally, Pauthenet et al. (2021) applied their analysis at 300 m at relatively shallow depths for the Weddell Sea, where the pycnocline extends deeper than 380 m (Thompson et al., 2018). As Fig. 4 has shown, the isopycnals are steeper in greater depth. It is therefore unclear if the shift in the minimum extent of 1.53° of the distance between the -0.7°C and -0.3°C isotherms at 300 m depth in winter during 2010-2014 of REF to a minimum extent of 5.41° in summer in 2096-2100 (Fig. S4b) is an effect of climate change and the shift in the front dynamics.

The decreasing wind strength over the 21st century in REF reduces the Ekman transport and downwelling above the continental shelf. Multiple studies have shown that a strengthening and poleward shift of the westerlies and a weakening of the easterly winds above the continental shelf will weaken the Ekman downwelling along the coast of the Weddell Sea (Spence et al., 2017; Naughten et al., 2021; Teske et al., 2024). The indirect influence of the wind strength on the flow of Antarctic Surface Water and mWDW onto the continental shelf has also been shown in previous studies (Hattermann et al., 2014; Dinniman et al., 2015; Haid et al., 2015; Hatterman, 2018). In particular, Hattermann et al. (2014) described the weakening of shallow and the strengthening of deep inflow towards the Fimbul ice shelf cavity in response to weaker easterly winds based on observations and modelling results. The projected reduced wind speed of the easterlies in our model towards the end of the 21st century and the southward shift of the mid-latitude westerlies, consistent with Spence et al. (2014) and Goyal et al. (2021), broaden the V-shaped density structure at the continental slope and reduce its depth in REF, as seen in Fig. 3. The uplift of the thermocline due to weakened downwelling lifts mWDW closer to the sill depth and slowly increases the amount of mWDW flowing into the Filchner Trough. A similar signature is found when comparing results from FECO with those from REF: The generally weaker wind speeds in the southern Weddell Sea in FECO than in REF weaken the Ekman downwelling further, reducing the V-shape depth in comparison to REF. The reduced density gradient weakens the barrier effect of the cross-slope gradient further and allows the strong cross-slope current to develop towards the end of the century that does not develop in REF.

4.2 Drivers of the accelerated density redistribution: cross-slope density gradient

One of the main criteria for the potential of the current system in the Filchner Trough to switch from a DSW-dominated state to the mWDW-dominated state is the density gradient across the Filchner Trough sill as has been previously shown (Ryan et al., 2017; Haid et al., 2023; Nissen et al., 2023). A near-bottom current of mWDW onto the continental shelf only develops once this gradient flattens out or reverses. Our results show that this on-shelf current disrupts the V-structure at the slope, reducing the V-shape to the upper 450 m of the water column and warming the Filchner Trough. The horizontal distance of the ASF (northern arm of the V-shape) to the continental slope varies over the year as shown in an analysis of observational data by Pauthenet et al. (2021). The introduction of the GOC provides a metric for the stability of the ASF in areas of cross-slope transport in dense-shelf areas. However, not all features of the V-shape of the ASF are included. The GOC is useful to detect strong changes in the cross-slope density distribution that remove the dip in the isopycnals or lead to a very large meridional displacement within the V-shape. What the GOC is not able to do, is to differentiate between a lot of small displacements that just exceed the distance threshold d_L and few very large meridional distances. Also, the selection of d_L as a maximum displacement before it reduces the GOC influences the result. A distance larger than ten times the grid size reduces the number of recognised events by 12.5% compared to a d_L of two times the grid size; with d_L 100 times the grid size, the number of recognised events decreases by 29.1%. The three-month delay between intensified cross-slope currents and a minimum event of the GOC at 250 m depth indicates a connection based on seasonal cross-slope water transport. Ryan et al. (2017) showed that during winter intensified DSW production and export suppress the isopycnals at the continental slope, reducing or stopping on-shore transport of mWDW. This conclusion is back up by the lack of correlation in FECO where DSW production is reduced

compared to REF. The lack of non-delayed correlation between cross-slope currents and the GOC indicates that an intensified bottom current does not destabilize the ASF in shallower than sill depth. This also implies that a (hypothetical) decreasing trend in the GOC cannot be regarded as an indicator that a cold-to-warm regime shift in Filchner Trough is about to occur in 360   the near future.

4.3 Comparison to other studies

Considering our results in the context of other scenario simulations for the 21st century, it becomes clear that the choice of atmospheric forcing data has a strong impact on the susceptibility of Filchner Trough to undergo a regime shift before 2100. Previous future projections produced a tipping of the Filchner Trough circulation in very high-emission scenarios (e.g., SSP5-365   8.5 or similar; Timmermann and Hellmer, 2013; Nissen et al., 2023) or idealized scenarios (e.g., 1pctCO2 scenario; Naughten et al., 2021). Ocean simulations with lower emission scenarios generally did not produce a regime shift (Timmermann and Hellmer, 2013; Nissen et al., 2023), except in case of a coupled atmospheric component (Teske et al., 2024, regime shift in SSP3-7.0 and SSP5-8.5 scenarios). While our reference simulation for the emission scenario SSP3-7.0 does not produce a regime shift during the 21st century, downscaling of the atmosphere in FECO induces a strong mWDW inflow before the end of 370   the 21st century. We therefore conclude that the potential for a regime shift in a warming climate in the SSP3-7.0 scenario might be higher than suggested by previous studies using relatively low-resolution atmospheric forcing (Nissen et al., 2023). With the currently implemented policies, global warming is projected to be between 2.2°C and 3.5°C by 2100, which corresponds to the warming projected for the SSP2-4.5 (2.1°C-3.5°C) and SSP3-7.0 (2.8°C-4.6°C) scenarios (Calvin et al., 2023). Our results thus highlight the importance of developing a better understanding of the potential implications for vulnerable climate components 375   like the Antarctic Slope Front and the Filchner Trough in the current climate development.

4.4 Limitations and caveats

Several studies have suggested that eddies play an important role in the transport of Circumpolar Deep Water across the continental shelf break (Nøst et al., 2011; Stewart and Thompson, 2015a). Our model is not eddy-resolving, but it has an eddy-permitting grid resolution on the Weddell Sea continental shelf (∼3-12 km). It has been proposed by Nøst et al. (2011) that 380   freshening of the shelf can lead to increased eddy kinetic energy which drives onshore cross-ASF eddy transport. The resolution of approx. 12 km at the continental slope in our model grid might lead to an underrepresentation of eddies, the Rossby radius in the southern Weddell Sea being 2-5 km. With reduced eddy presence, the model might underestimate cross-slope volume transport. An underrepresentation of eddy-driven on-shore transport of mWDW would mean a greater depth of the V-shape as the lack of mesoscale eddies reduces the relaxation of the isopycnals above the continental slope (Dettling et al., 2024). 385   As a result, the temperatures on the continental shelf would be underestimated. A shallower V-shape at the continental slope in a simulation with an adequate eddy representation might lead to an earlier regime shift of the Filchner Trough due to the lower density gradient into the shelf and the higher connectivity between the slope current and the Filchner Trough through the sloping isopycnals.

5   Conclusions

390   We have presented model results indicating the future evolution of the density distribution across the Filchner Trough sill, a key property of the Antarctic Slope Front in the Southern Weddell Sea. The reference simulation REF and the experiment simulation FECO with down-scaled atmospheric forcing both reproduce the typical V-shaped density distribution that is formed by interplay of Ekman downwelling and Dense Shelf Water export in the southern Weddell Sea. Sea ice loss in the warming climate of the SSP3-7.0 emission scenario decreases the density on the continental shelf and flattens the southern arm of the

395   V-shape in REF and FECO. This causes an increased sensitivity of the density distribution on the continental shelf to seasonal wind speed variations. Using results from a regional, high-resolution atmosphere model as forcing, we find an acceleration of the density redistribution on the continental shelf, which leads to a regime shift with modified Warm Deep Water entering Filchner Trough before the end of the 21st century for the high emission scenario SSP3-7.0. Colder air temperatures in the multi-year mean are more than outweighed by the warmer summer air temperatures of the regionally down-scaled atmosphere,

400   accelerating density loss on the continental shelf, which ultimately leads to a regime shift from a cold Dense Shelf Water dominated Filchner Trough to a warm, modified Warm Deep Water dominated trough in 2093. The criterion of spatial coherency of the V-shape along the continental slope, quantified by the grade of connectivity, is not usable as a tool to predict an imminent regime shift because the southward transport of modified Warm Deep Water is, contrary to our expectations, not a result of a weakening of the slope front, but instead leads to a temporary disturbance of the ASF and the associated V-shape. While

405   the density minimum is completely restored after disruption in present-day climate, in a warming climate the distinct V-shape remains confined to the upper ocean. Due to the geostrophic nature of the Antarctic Slope Current, the flattening of the northern arm of the V-shape and stronger seasonality will affect the transport of the slope current and the transport of heat towards the peninsula and onto the continental shelf in the future.

The accelerated density redistribution by the high-resolution atmospheric data and the resulting regime shift show that

410   the potential for a regime shift in the Filchner Trough in the SSP3-7.0 scenarios is higher than previously published ocean simulations of the same scenario suggest. With the current climate policies, the projected 21st-century global warming lies within the potential range of the SSP3-7.0 scenario, increasing the urgency to better understand and represent vulnerable climate components.

Code and data availability.   The code for FESOM can be accessed from the esm-tool at https://github.com/esm-tools/esm_tools (last access

415   01.08.2024). The Matlab codes used for the analysis of the model output will be made available upon request to the corresponding author.

The CCLM model is available from the CCLM community website: https://clmcom.scrollhelp.site/clm-community (last access: 07 August 2024). CCLM data are available in the DKRZ long-term archive: https://hdl.handle.net/21.14106/cb44f718061ed8e9cdeb574d51113b64ec781564 (last access: 07 August 2024, (Zentek and Heinemann, 2023)).

Author contributions. VT ran the FESOM simulations, conducted the analyses, and prepared the figures. CN and VT prepared the FESOM

420   model code. GH and RZ prepared the CCLM model code and ran the simulations. VT, RT and TS contributed to the interpretation of the

results. All authors contributed to the writing and editing of the manuscript.

Competing interests. The authors declare no competing interests.

Acknowledgements. This work was funded by Deutsche Forschungsgemeinschaft SPP 1158 under grants SE2901/2, HE2740/33 and TI296/9.

CCLM simulations used resources of the Deutsches Klimarechenzentrum (DKRZ) granted by its Scientific Steering Committee (WLA) under

425   project ID bb0958.

References

Årthun, M., Nicholls, K.-W., Makinson, K., Fedak, M.-A., and Boehme, L.: Seasonal inflow of warm water onto the southern Weddell Sea continental shelf, Antarctica, Geophysical Research Letters, 39(17), 2–7, https://doi.org/10.1029/2012GL052856, 2012.

Baines, P.: A model for the structure of the Antarctic Slope Front, Deep Sea Research Part II: Topcial Studies in Oceanography, 56, 859–873, 2009.

Beadling, R. L., Krasting, J. P., Griffies, S. M., Hurlin, W. J., Bronselaer, B., Russell, J. L., MacGilchrist, G. A., Tesdal, J., and Winton, M.: Importance of the Antarctic Slope Current in the Southern Ocean Response to Ice Sheet Melt and Wind Stress Change, Journal of Geophysical Research: Oceans, 127, e2021JC017 608, 2022.

Calvin, K., Dasgupta, D., Krinner, G., Mukherji, A., Thorne, P. W., Trisos, C., Romero, J., Aldunce, P., Barrett, K., Blanco, G., Cheung, W. W., Connors, S., Denton, F., Diongue-Niang, A., Dodman, D., Garschagen, M., Geden, O., Hayward, B., Jones, C., Jotzo, F., Krug, T., Lasco, R., Lee, Y.-Y., Masson-Delmotte, V., Meinshausen, M., Mintenbeck, K., Mokssit, A., Otto, F. E., Pathak, M., Pirani, A., Poloczanska, E., Pörtner, H.-O., Revi, A., Roberts, D. C., Roy, J., Ruane, A. C., Skea, J., Shukla, P. R., Slade, R., Slangen, A., Sokona, Y., Sörensson, A. A., Tignor, M., van Vuuren, D., Wei, Y.-M., Winkler, H., Zhai, P., Zommers, Z., Hourcade, J.-C., Johnson, F. X., Pachauri, S., Simpson, N. P., Singh, C., Thomas, A., Totin, E., Alegría, A., Armour, K., Bednar-Friedl, B., Blok, K., Cissé, G., Dentener, F., Eriksen, S., Fischer, E., Garner, G., Guivarch, C., Haasnoot, M., Hansen, G., Hauser, M., Hawkins, E., Hermans, T., Kopp, R., Leprince-Ringuet, N., Lewis, J., Ley, D., Ludden, C., Niamir, L., Nicholls, Z., Some, S., Szopa, S., Trewin, B., van der Wijst, K.-I., Winter, G., Witting, M., Birt, A., and Ha, M.: IPCC, 2023: Climate Change 2023: Synthesis Report. Contribution of Working Groups I, II and III to the Sixth Assessment Report of the Intergovernmental Panel on Climate Change [Core Writing Team, H. Lee and J. Romero (eds.)]. IPCC, Geneva, Switzerland., Tech. rep., Intergovernmental Panel on Climate Change, https://doi.org/10.59327/IPCC/AR6-9789291691647, 2023.

Cape, M. R., Vernet, M., Skvarca, P., Marinsek, S., Scambos, T., and Domack, E.: Foehn winds link climate-driven warming to ice shelf evolution in Antarctica, Journal of Geophysical Research: Atmosphere, 120, https://doi.org/10.1002/2015JD023465, 2015.

Daae, K., Hattermann, T., Darelius, E., Mueller, R., Naughten, K. A., and Timmermann, R. e. a.: Necessary Conditions for Warm Inflow Toward the Filchner Ice Shelf, Weddell Sea, Geophysical Research Letters, 47(22), e2020GL089 237, https://doi.org/10.1029/2020GL089237, 2020.

Danilov, S., Wang, Q., Timmermann, R., Iakovlev, N., Sidorenko, D., Kimmritz, M., Jung, T., and Schröter, J.: Finite-Element Sea Ice Model (FESIM), version 2, Geoscientific Model Development, pp. 1747–1761, 2015.

Darelius, E., Fer, I., and Nicholls, K.-W.: Observed vulnerability of Filchner-Ronne Ice Shelf to wind-driven inflow of warm deep water, Nature Communications, 7, 1–7, https://doi.org/10.1038/ncomms12300, 2016.

Dettling, N., Losch, M., Pollmann, F., and Kanzow, T.: Toward Parameterizing Eddy-Mediated Transport of Warm Deep Water across the Weddell Sea Continental Slope, Journal of Physical Oceanography, 54, 2024.

Dinniman, M., Klinck, J., Bai, L.-S., Bromwich, D., Hines, K. M., and Holland, D.: The effect of atmospheric forcing resolution on the delivery of ocean heat to the Antarctic floating ice shelves, Journal of Climate, pp. 6067–6085, https://doi.org/10.1175/JCLI-D-14-00374. 1, 2015.

Dinniman, M. S., Klinck, J. M., and Hofmann, E. E.: Sensitivity of Circumpolar Deep Water Transport and Ice Shelf Basal Melt along the West Antarctic Peninsula to Changes in the Winds, Journal of Climate, 2012, 4799–4816, 2012.

Elvidge, A., Renfrew, I., King, J., Orr, A., and Lachlan-Cope, T.: Foehn warming distributions in non-linear and linear flow regimes: A focus on the Antarctic Peninsula, Quarterly Journal of the Royal Meteorological Society, 142, https://doi.org/10.1002/qj.2489, 2014.

Foldvik, A., Gammelsrø d, T., and Torresen, T.: Circulation and Water Masses on the Southern Weddell Sea Shelf, Oceanology of the Antarctic Continental Shelf, 43, 5–20, 1985.

465   Gill, A.: Circulation and bottom water production in the Weddell Sea, Deep-Sea Research and Oceanographic Abstracts, 20, 111–140, 1973.

Goyal, R., Sen Gupta, A., Jucker, M., and England, M. H.: Historical and Projected Changes in the Southern Hemisphere Surface Westerlies, Geophysical Research Letters, 48, 1–13, 2021.

Graham, J., Heywood, C., Chavanne, C. P., and Holland, P. R.: Seasonal variability of water masses and transport on the Antarctic continental shelf and slope in the southeastern Weddell Sea, Journal of Geophysical Research: Oceans, 118, 2201–2214, 2013.

470   Gurses, O., Kolatschek, V., Wang, Q., and Rodehacke, C. B.: Brief communication: A submarine wall protecting the Amundsen Sea intensifies melting of neighboring ice shelves, The Cryosphere, 13, 2317–2324, https://doi.org/10.5194/tc-13-2317-2019, 2019.

Haid, V., Timmermann, R., Ebner, L., and Heinemann, G.: Atmospheric forcing of coastal polynyas in the southwestern Weddell Sea, Antarctic Science, 27, 388–402, https://doi.org/10.1017/S0954102014000893, 2015.

Haid, V., Timmermann, R., Gurses, O., and Hellmer, H. H.: On the drivers of regime shifts in the Antarctic marginal seas, exemplified by the
475   Weddell Sea, Ocean Science, 19, 1529–1544, https://doi.org/10.5194/os-19-1529-2023, 2023.

Hatterman, T.: Antarctic thermocline dynamics along a narrow shelf with easterly winds, Journal of Physical Oceanography, 48(10), 2419–2443, https://doi.org/10.1175/JPO-D-18-0064.1, 2018.

Hattermann, T.: Antarctic thermocline dynamics along a narrow shelf with easterly winds, Journal of Physical Oceanography, 48, 2419–2443, 2018.

480   Hattermann, T., Smedsrud, L. H., Nøst, O. A., Lilly, J. M., and Galton-Fenzi, B. K.: Eddy-resolving simulations of the Fimbul Ice Shelf cavity circulation: Basal melting and exchange with open ocean, Ocean Modelling, 82, 28–44, 2014.

Heinemann, G., Schefczyk, L., Willmes, S., and Shupe, M. D.: Evaluation of simulations of near-surface variables using the regional climate model CCLM for the MOSAiC winter period, Elementa: Science of the Anthropocene, 10, 1–22, 2022.

Hellmer, H. H. and Olbers, D. J.: A two-dimensional model for the thermohaline circulation under an ice shelf, Antarctic Science, 1, 325–336,
485   https://doi.org/10.1017/S0954102089000490, 1989.

Hellmer, H. H., Kauker, F., Timmermann, R., Determann, J., and Rae, J.: Twenty-first-century warming of a large Antarctic ice-shelf cavity by a redirected coastal current, Nature, 485(7397), 225–228, https://doi.org/10.1038/nature11064, 2012.

Hellmer, H. H., Kauker, F., Timmermann, R., , and Hattermann, T.: The fate of the Southern Weddell sea continental shelf in a warming climate, Journal of Climate, 30(12), 4337–4350, https://doi.org/10.1175/JCLI-D-16-0420.1, 2017.

490   Heywood, K. J., Schmidtko, S., Heuzé, C., Kaiser, J., Jickells, T. D., Queste, B. Y., Stevens, D. P., Wadley, M., Thompson, A. F., Fielding, S., Guihen, D., Creed, E., Ridley, J. K., and Smith, W.: Ocean processes at the Antarctic continental slope, Philosophical Transactions of the Royal Society A, 372, 20130 047, https://doi.org/10.1098/rsta.2013.0047, 2014.

Holland, D. M. and Jenkins, A.: Modeling Thermodynamic Ice–Ocean Interactions at the Base of an Ice Shelf, Journal of Physical Oceanography, 29, 1787–1800, https://doi.org/10.1175/1520-0485(1999)029<1787:MTIOIA>2.0.CO;2, 1999.

495   Huneke, W. G. C., Morrison, A. K., and Hogg, A. M.: Spatial and Subannual Variability of the Antarctic Slope Current in an Eddying Ocean–Sea Ice Model, Journal of Physical Oceanography, 52, 347–361, 2022.

Kida, S.: The impact of open oceanic processes on the Antarctic Bottom Water outflows, Journal of Physical Oceanography, 41, 1941–1957, 2011.

Le Paih, N., Hattermann, T., Boebel, O., Kanzow, T., Lüpkes, C., Rohardt, G., Strass, V., and Herbette, S.: Coherent Seasonal Acceleration
500   of the Weddell Sea Boundary Current System Driven by Upstream Winds, Journal of Geophysical Research: Oceans, 125, 1–20, 2020.

Lockwood, J. W., Dufour, C. O., Griffies, S. M., and Winton, M.: On the Role of the Antarctic Slope Front on the Occurrence of the Weddell Sea Polynya under Climate Change, Journal of Climate, 34, 2529–2548, 2021.

Mathiot, P., Goosse, H., Fichefet, T., Barnier, B., and Gallée, H.: Modelling the seasonal variability of the Antarctic Slope Current, Ocean Science, 7, 455–470, 2011.

505 Meinshausen, M., Nicholls, Z. R., Lewis, J., Gidden, M. J., Vogel, E., and Freund, M. e. a.: The shared socio-economic pathway (SSP) greenhouse gas concentrations and their extensions to 2500, Geoscientific Model Development, 13(8), 3571–3605, https://doi.org10.5194/gmd-13-3571-2020, 2020.

Naughten, K. A., De Rydt, J., Rosier, S. H. R., Jenkins, A., Holland, P. R., and Ridley, J. K.: Two-timescale response of a large Antarctic ice shelf to climate change, Nature Communications, 12(1), 1–10, https://doi.org/10.1038/s41467-021-22259-0, 2021.

510 Nissen, C., Timmermann, R., Hoppema, M., Gürses, Ö., and Hauck, J.: Abruptly attenuated carbon sequestration with Weddell Sea dense waters by 2100, Nature Communications, 13, 2022.

Nissen, C., Timmermann, R., Hoppema, M., and Hauck, J.: A regime shift on Weddell Sea Continental Shelves with Local and Remove Physical and Biogeochemical Implications is Avoidable in a 2°C Scenario, Journal of Climate, 36, 6613–6630, 2023.

Nissen, C., Timmermann, R., van Caspel, M., and Wekerle, C.: Altered Weddell Sea warm- and dense-water pathways in response to 21st-515 century climate change, Ocean Science, 20, 85–101, https://doi.org/10.5194/os-20-85-2024, 2024.

Nøst, O., Biuw, M., Tverberg, V., Lydersen, C., Hattermann, T., Zhou, Q., Smedsrud, L. H., , and Kovacs, K. M.: Eddy overturning of the Antarctic Slope Front controls glacial melting in the Eastern Weddell Sea, Journal of Geophysical Research, 116(C11014), 1–17, https://doi.org.de/10.1029/2011JC006965, 2011.

Ong, E. Q. Y., Doddridge, E., Constantinou, N. C., Hogg, A. M., and England, M. H.: Intrinsically Episodic Antarctic Shelf Intrusions of 520 Circumpolar Deep Water via Canyons, Journal of Physical Oceanography, 54, 1195–1210, 2023.

Ou, H.: Watermass Properties of the Antarctic Slope Front: A Simple Model, Journal of Physical Oceanography, 37, 50–59, 2007.

Pauthenet, E., Sallée, J. B., Schmidtko, S., and Nerini, D.: Seasonal variation of the antarctic slope front occurrence and position estimated from an interpolated hydrographic climatology, Journal of Physical Oceanography, 51, 1539–1557, 2021.

Peña-Molino, B., McCartney, M. S., and Rintoul, S. R.: Direct observations of the Antarctic Slope Current transport at 113°E, Journal of 525 Geophysical Research: Oceans, 121, 7390–7407, 2016.

Ryan, S., Hattermann, T., Darelius, E., , and Schröder, M.: Seasonal cycle of hydrography on the eastern shelf of the Filchner Trough, Weddell Sea, Antarctica, Journal of Geophysical Research: Oceans, 122(8), 6437–6453, https://doi.org/10.1002/2017JC012916, 2017.

Ryan, S., Hellmer, H. H., Janout, M., Darelius, E., Vignes, L., and Schröder, M.: Exceptionally Warm and Prolonged Flow of Warm Deep Water Toward the Filchner-Ronne Ice Shelf in 2017, Geophysical Research Letters, 47(13), 1–10, https://doi.org/10.1029/2020GL088119, 530 2020.

Schmidtko, S., Heywood, K. J., Thompson, A. F., , and Aoki, S.: Multidecadal warming of Antarctic waters, Science, 346(6214), 1227–1232, https://doi.org/10.1126/science.1256117, 2014.

Semmler, T., Danilov, S., Gierz, P., Goessling, H. F., Hegewald, J., and Hinrichs, C. e. a.: Simulations for CMIP6 With the AWI Climate Model AWI-CM-1-1, Journal of Advances in Modeling Earth Systems, 12(9), 1–34, https://doi.org/10.1029/2019MS002009, 2020.

535 Spence, P., Griffies, S. M., England, M. H., Hogg, A. M., Saenko, O. A., and Jourdain, N. C.: Rapid subsurface warming and circulation changes of Antarctic Coastal waters by poleward shifting winds, Geophysical Research Letters, 41, 4601–4610, 2014.

Spence, P., Holmes, R. M., Hogg, A. M., Griffies, S. M., Stewart, K. D., and England, M. H.: Localized rapid warming of West Antarctic subsurface waters by remote winds, Nature Climate Change, 7, 595–603, 2017.

St-Laurent, P., Klinck, J. M., and Dinniman, M. S.: On the role of coastal troughs in the circulation of warm circumpolar deep water on Antarctic shelves, Journal of Physical Oceanography, 43, 51–64, 2013.

Steger, C. and Bucchignani, E.: Regional Climate Modelling with COSMO-CLM: History and Perspectives, Atmosphere, 11, 2020.

Stewart, A. and Thompson, A.: Eddy-mediated transport of warm Circumpolar Deep Water cross the Antarctic Shelf Break, Geophysical Research Letters, 42, 432–440, 2015a.

Stewart, A. and Thompson, A.: The Neutral Density Temporal Redidual Mean overturning circulation, Ocean Modelling, 90, 44–56, 2015b.

Stewart, A., Klocker, A., and Menemenlis, D.: Acceleration and Overturning of the Antarctic Slope Current by Winds, Eddies, and Tides, Journal of Physical Oceanography, 49, 2043–2074, 2019.

Sverdrup, H.: The Currents off the Coast of Queen Maud Land, Norsk Geografisk Tidsskrift - Norwegian Journal of Geography, 14, 1954.

Teske, V., Timmermann, R., and Semmler, T.: Subsurface warming in the Antarctica's Weddell Sea can be avoided by reaching the 2°C warming target, Communications Earth & Environment, 5, 93, 2024.

Thompson, A. F., Stewart, A. L., Spence, P., and Heywood, K. J.: The Antarctic Slope Current in a Changing Climate, Reviews of Geophysics, 56, 741–770, 2018.

Timmermann, R. and Goeller, S.: Response to Filchner-Ronne Ice Shelf cavity warming in a coupled ocean-ice sheet model - Part 1: The ocean perspective, Ocean Science, 13(5), 765–776, https://doi.org/10.5194/os-13-765-2017, 2017.

Timmermann, R. and Hellmer, H. H.: Southern Ocean warming and icreased ice shelf basal melting in the twenty-first and twenty-second centuries based on coupled ice-ocean finite-element modelling, Ocean Dynamics, 63(9-10), 1011–1026, https://doi.org/10.1007/s10236-013-0642-0, 2013.

Timmermann, R., Wang, Q., and Hellmer, H.: Ice-shelf basal melting in a global finite-element sea-ice/ice-shelf/ocean model, Ann. Glaciol., 53, 303–314, 2012.

Van Lipzig, N. P. M., King, J. C., Lachlan-Cope, T. A., and van den Broeke, M. R.: Precipitation, sublimation, and snow drift in the Antarctic Peninsula region from a regional atmospheric model, Journal of Geophysical Research, 109, D24 106, https://doi.org/10.1029/2004JD004701, 2004.

Van Wessem, J. M., Reijmer, C. H., van de Berg, W. J., van den Broeke, M. R., J., C. A., van Ulft, L. H. E., and van Meijgaard, E.: Temperature and Wind Climate of the Antarctic Peninsula as Simulated by a High-Resolution Regional Atmospheric Climate Model, Journal of Climate, 28, 1831–1844, 2015.

Wang, Q., Danilov, S., Sidorenko, D., Timmermann, R., Wekerle, C., and Wang, X. e. a.: The Finite Element Sea Ice-Ocean Model (FESOM) v.1.4: Formulation of an ocean general circulation model, Geoscientific Model Development, 7(2), 663–693, https://doi.org/10.1175/JCLI-D-16-0420.1, 2014.

Zentek, R. and Heinemann, G.: Verification of the regional atmospheric model CCLM v5.0 with conventional data and Lidar measurements in Antarctica, Geosci. Model Dev, 13, 1809–1825, 2020.

Zentek, R. and Heinemann, G.: COSMO-CLM REDOCCA Simulation (Version 2), https://hdl.handle.net/21.14106/cb44f718061ed8e9cdeb574d51113b64ec781564, 2023.